Technical Note
radphi-1999-601

Predicted Rates in Radphi following the Barrel Upgrade

Richard Jones
University of Connecticut, Storrs, CT

June 16, 1999
(updated July 2, 1999)

Abstract

During the first half of 1999 the Radphi experiment underwent a major upgrade in which the recoil proton detector was replaced by a scintillator hodoscope covering angles from 30^o to 90^o in the lab, and a barrel calorimeter was added. By increasing the detector coverage both for the recoil proton and for gammas in the barrel, the experiment improves both its acceptance and its ability to discriminate background from signal events. The increase in acceptance comes at a cost of increased trigger rates and data acquisition overhead, which can offset the gains by requiring the experiment to run at lower intensity or higher dead time. This is a major concern to Radphi, whose primary physics goals require obtaining the highest statistics possible. This note summarizes what we expect for the increase in trigger rates in the upgraded detector, based upon Monte Carlo simulation.

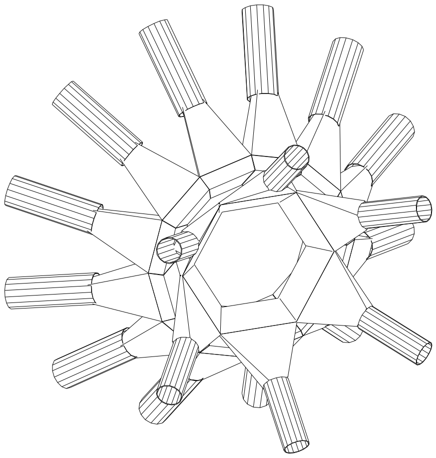

Figure 1: Drawing of the Radphi recoil proton trigger scintillators that are being replaced by a new barrel assembly during the barrel upgrade.

1 Introduction

From data taken during parasitic running in the summer of 1998, the Radphi experiment has demonstrated its capability to trigger on and reconstruct multi-photon final states up to the mass of the $\phi(1020)$. The most significant obstacle that we encountered to our readiness for our first physics run is the rate limitations of our trigger and data acquisition. The rates expected for the looked-for ϕ radiative decays are very low. When running at $5 \cdot 10^7$ γ/s, near the highest photon beam intensity compatible with tagging, we expect of order 1 event per hour per rare decay channel. At this beam intensity, the total rate of hadronic events coming from the target is calculated to be about 170KHz. Scaling measurements taken during 1998 parasitic tests up to this beam intensity yield a total rate of $8.5 \cdot 10^7$/s charged particles within the acceptance of the detector.

The experiment is looking for final states of nγ plus a recoil proton, so most of the background rate can be excluded fairly easily. The basic trigger design is to look for a single charged track at large angle that corresponds to the kinematics of the recoil proton, and then look in the forward calorimeter for a large energy deposition. The trigger has gone through several revisions, based upon experience gained during parasitic running, and we now have a design capable of collecting data efficiently at our design beam intensity of $5 \cdot 10^7$ tagged γ/s. Following a brief commissioning of the new trigger hardware, we would be ready now to take physics data with the existing detector as soon as we can get a place on the schedule.

The interval from the time that an approved experiment is ready until the time it can receive beam as primary user is presently a year or more. In view of this, the Radphi collaboration decided to proceed immediately with its plans to upgrade the barrel region of the detector. The upgrade extends the photon coverage from the 28^o back to 90^o in the lab by adding a barrel calorimeter, and also increases the angular acceptance of the recoil proton trigger. This was accomplished by replacing the recoil proton detector [RPD] shown in Fig. 1 with the barrel calorimeter and scintillator assembly from the former Jetset experiment (PS-202 CERN-LEAR) shown in Fig. 2.

This upgrade significantly improves the quality of the experiment, increasing the acceptance for ϕ radiative decay channels to the a_0 and f_0 channels by more than a factor of 2, and significantly improving our ability to discriminate these reactions from background. It also represents a major change to the configuration under which we have run in the past, and so will require some additional commissioning time.

This point was noted by the Jefferson Lab review committee during our readiness review that was held

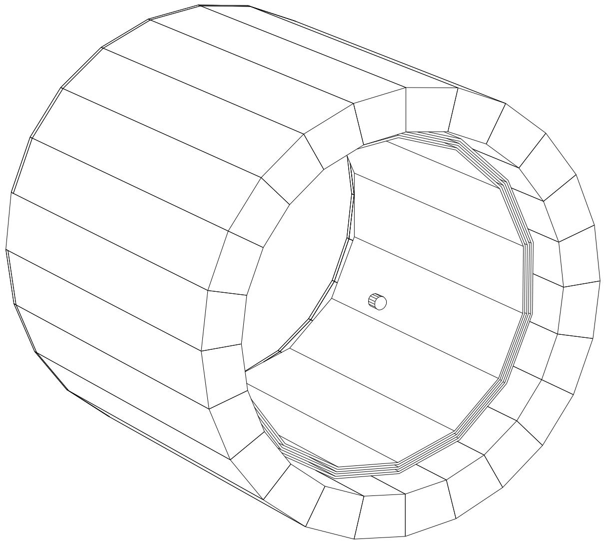

Figure 2: Drawing of the new barrel assembly being installed in the Radphi experiment during the barrel upgrade.

on March 10, 1999. We asked to be placed on the schedule nevertheless, based upon the fact that the upgrade mainly adds new capability without affecting present function (apart from the trigger) and that this apparatus has been used successfully in a prior experiment. The committee went along with our request to place us on the tentative schedule for the year 2000, but made some conditions related to commissioning the upgraded detector during summer 1999 parasitic running. In particular, they requested that we calculate the rates that we expect in the detector trigger elements under the new configuration in advance of test beam. Subsequent measurement of rates during 1999 parasitic running in agreement with these predictions would confirm our claim that we understand the apparatus and operating conditions of the experiment.

The most important risk in the upgrade, as pointed out above, is the change that it makes to the trigger. Instead of covering a narrow annulus between 40^o and 60^o, the barrel scintillators now subtend the region from 32^o to just beyond 90^o. This increased acceptance, particularly towards forward angles, may be expected to result in an increased rate of level-1 triggers and introduce new dead time to the system. The major conclusion of this study is that the total level-1 rate is expected to decrease, rather than increase, in the new configuration, and at the same time running with higher acceptance in the recoil proton by a factor of 2.

2 Method

This study was performed using *Gradphi* [2], a Monte Carlo simulation of the Radphi apparatus based upon the *GEANT* package. The simulation begins with an electron from the primary beam entering the bremsstrahlung radiator. After the radiator, the electron is removed and the simulation continues to follow the photon produced. Bremsstrahlung is generated between a lower cutoff of 1MeV and the end point, and has the proper angular distribution. The photon beam passes through the primary collimator, a pair of sweeping magnets and a secondary collimator before arriving at the CLAS target. Interactions are simulated whenever photons pass through matter and interact. Downstream of the CLAS target, the remaining photons pass through an exit window into a helium tube which passes through the forward aperture in CLAS and down to the alcove area. At the entrance to the alcove the helium tube passes through the lead "doughnut" that defines the beam aperture for this experiment, through the lead shielding wall and on to within a few cm of the target. There the photons remaining in the beam exit through a window into air and then pass into the target if they are within its radius. Downstream of the target, particles are tracked until they either enter a calorimeter block, reach the back wall of the alcove, or fall below the kinetic energy cutoff of 1MeV. Any secondaries generated by interactions or decays are also followed by the simulation. All of the interactions that GEANT knows about are simulated, including for photons electron pair production, Compton scattering and the photoelectric effect, and for electrons ionization energy loss, multiple scattering, bremsstrahlung and annihilation (for positrons).

Hadronic interactions for all particles are included using the *GHEISHA* package. The hadronic interactions are parameterizations of cross sections with a range of validity usually limited to high energies or averages over an ensemble of low-energy particles such as characterizes the response of a hadronic calorimeter. The electromagnetic part of the GEANT simulation is quite detailed, however, and generally reliable at energies above 1MeV down to the level of a few percent in its cross sections and angular distributions. Care was taken in the geometrical description of the experimental setup that is used by *Gradphi* to put in any elements that might affect the simulation at the percent level. The dimensions and distances between detector elements in the simulation are accurate to 5% or better. Based upon this and the observation that the detector rates are dominated by electromagnetic background, the systematic error for the simulation may be estimated to be at the level of 5%.

3 Results

Three separate Monte Carlo simulations were run for this study. Run 1998 was done under the conditions of the experiment during parasitic running the summer of 1998 at 4GeV end point energy. These numbers may be directly compared with the rates measured during that period, and provide a consistency check of the simulation. Run 1999a was done under the conditions expected for summer 1999 parasitic running at 5.5GeV end point energy. Run 1999b was done under similar conditions as 1999a, except that the Radphi target was moved 2m downstream from its nominal position. This places the target beyond the front face of the glass, and so provides an estimate of the rates component that does not come from the target. The target was not removed entirely for run 1999b because the flux at the face of the target is used in the simulation to normalize the bremsstrahlung flux in lieu of simulating the tagger. The major results of these runs are shown in Table 1. For each run two numbers are given for the rates in each detector: the first is the total number of hits and the second is the total number of events with at least one hit. The former corresponds to the sum of scalers connected to each channel and the latter to the scaler counting the logical *or* for the entire detector.

The UPV is a plane of scintillators located upstream of the target that serves to veto beam halo events. The CPV is a plane of scintillators located between the target and the forward calorimeter which serves to veto any events containing forward-going charged tracks. Both the CPV and UPV have a rectangular hole in the center where the beam passes. The barrel scintillator detector [BSD] consists of three concentric cylinders of 5mm thick scintillator paddles. The three layers are labelled in Table 1 as layers 1 (inner) 2 (middle) and 3 (outer). The data in Table 1 show several important things regarding the background.

1. Increasing the beam end point energy from 4GeV to 5.5GeV has very little affect on the CPV rate. It will run in 1999 at substantially the same rate as it did in 1998, for comparable beam intensity.

2. The background is largely low-energy particles. This can be seen from the fact that the outer layers of the BSD are effectively shielded by the material of those inside, even though the layers are composed of only 5mm of plastic scintillator.

3. Roughly 90% of the background within the detector acceptance is coming from the target. This can be seen by comparing column 2 (target in) with column 3 (target out). The UPV is located upstream of the target, and so its rates are largely unaffected when the target is removed, but the CPV and BSD rates go down by about a factor of 10.

4. The residual background in the detector when the target is removed is coming from the lead collimator, and has a harder energy spectrum than the target-related background. This can be seen from the fact that rates are roughly the same in all three BSD layers when the target is removed. That these particles are coming from the region of the collimator was seen by examining events during the simulation.

5. With the UPV moved upstream in the 1999 runs relative to its position during 1998, its rate is substantially decreased. It still has a role even in its far-upstream position, however, because about half of the 640 halo tracks that fire the BSD triple coincidence also hit the UPV. In the following

Table 1: Hit statistics from Monte Carlo simulation. Run 1998 simulates conditions during parasitic running in the summer of 1998 at 4GeV end point energy; run 1999a simulates conditions expected during parasitic running in the summer of 1999 at 5.5GeV end point with the Radphi target in place, and 1999b the same but with the target effectively removed.

	1998		1999a		1999b	
total simulated	10.6 M		10.6 M		10.6 M	
total hit target	8.00 M		8.89 M		8.65 M	
total tagged	172 K		167 K		167 K	
tagged hit target	142 K		149 K		145 K	
UPV rate, *or*	6850	6530	1660	1360	1750	1380
CPV rate, *or*	238 K	182 K	234 K	178 K	16.7 K	13.7 K
BSD rate, *or* for layer 1			29.2 K	26.1 K	1830	1290
BSD rate, *or* for layer 2			15.2 K	13.7 K	1700	1230
BSD rate, *or* for layer 3			9210	8140	1710	1190
BSD rate for triple coinc.			7370		640	

Table 2: Comparison between rates in the trigger counters predicted by Monte Carlo run 1998 with measured rates from summer 1998 parasitic running. Both data and Monte Carlo have been normalized to 10 MHz in the tagger range from 78% to 95% of the bremsstrahlung spectrum. The data have been corrected for electronics dead time.

	Monte Carlo	measurement
UPV *or*	380 K	720 K
CPV *or*	11 M	14 M
RPD *or*	(150 K)	75 K

discussion I will show that it will be possible to reduce the BSD triple-coincidence rate down to a level where the UPV veto may be useful.

Table 2 compares the calculated rates from run 1998 with those measured during summer 1998 parasitic running. The relative normalization was fixed by scaling both measured rates and Monte Carlo to a common beam intensity of 10^7 tagged γ/s. This value corresponds to the *tagger-OR*, not the rate of tagged photons that hit the Radphi target per second. The rates in the CPV and UPV can be directly compared with the Monte Carlo. The Monte Carlo did not include a description of the RPD, but a rough comparison can be made between the measured RPD rate and the Monte Carlo rate in the barrel scintillators between the polar angles of 40^o and 60^o. This value is shown in parentheses in Table 2 because the equivalence to the RPD is only approximate. The comparison with the measured RPD rate is also affected by the fact that the discriminators on the thick (E) RPD counters were set somewhat above the minimum ionizing peak. This was done to reduce the trigger rate from electromagnetic background while retaining good efficiency for the more heavily ionizing recoil protons. With these considerations taken into account, the Monte Carlo and measured RPD rates in Table 2 are compatible.

The measured rate of the UPV *or* shown in Table 2 is an average value over the 1998 run period. It varied from the value shown by a factor of about 2, depending on the tune of the machine. The value shown in Table 2 as measurement represents an effective average over periods of stable operation. Because it is located upstream of the Radphi target, the UPV is more sensitive to the quality of the beam than are the other elements of the detector. The difference between measured and simulated rates in the UPV might be explained by non-ideal alignment and transverse profile of the electron beam. The simulation assumes ideal alignment and zero emittance for the electron beam. The Monte Carlo value should be taken as a lower bound for the UPV (under 1998 conditions) while the CLAS target is full.

The CPV *or* provides the most rigorous test of the Monte Carlo. The thresholds for these counters were set low to obtain good efficiency for all charged particles. In the Monte Carlo energy loss spectrum, the minimum ionizing edge is readily seen and summing the count rate is not ambiguous. The rate is dominated by soft e^+/e^- tracks coming from beam interactions in the target, and so is not very sensitive to effects related to beam quality of the kind discussed above for the UPV. I would expect the simulation and measured rates to agree within about 5%. Small variations in the Monte Carlo CPV rate at the level of a few percent are obtained by adjusting the parameters of the simulation (changing the low-energy cutoff in the tracking, generating bremsstrahlung all the way down to the KeV regime, enabling discrete delta-ray production) but at the 5% level the Monte Carlo prediction appears solid.

If, instead of taking the CPV *or* rate from Table 1 to compare with the measurement, we take the total CPV rate then the agreement is excellent. The difference between the total rate and the *or* rate is that the total rate counts all hits separately while the *or* only counts the number of events with at least one hit. On paper, the electronics that generated the CPV *or* during 1998 running should count only once no matter how many tracks there are, provided that all of the hits are within 5ns of each other. The simulation shows essentially all hits associated with a single beam photon as coming within 5ns of each other. The signals from individual CPV paddles were synchronized to within 3ns of each other, and dispersion from light propagation delays down the paddles is not a large enough effect to explain the difference. Double-pulsing in the CPV discriminators might have been responsible, but that will have to be checked during the next run.

For the purposes of this report it suffices that the numbers from the simulation agree to within 20% with those that were measured during 1998 parasitic running. Based upon that we are able to forecast the trigger rates for 1999 with sufficient accuracy to show that the level 1 rate with the upgraded detector will be the same or even lower than was obtained with the RPD, for more than twice the acceptance. With the trigger and data acquisition improvements in place this year, we expect to demonstrate efficient operation of Radphi at the design intensity during the summer 1999 g6 run period.

4 Level-1 Trigger

The Monte Carlo value of 150 KHz shown in Table 2 for the total charged flux within the angular range from 40^o to 60^o is about 1/3 of the total rate between 32^o and 90^o that is seen by the BSD. Thus there is a factor of 6 higher level-1 trigger rate with the BSD triple coincidence than was obtained in 1998 with the RPD. However this comparison is not fair because the RPD rate contains a significant reduction from raising the threshold above the minimum ionizing edge. This technique should also work for the BSD. In order to evaluate how effective this can be in reducing the level-1 rate, a sample of recoil protons in the BSD is needed. Knowing the pulse height spectrum of recoil protons, one can then adjust the threshold to optimize between rejection of minimum-ionizing background and efficient collection of the desired events.

A Monte Carlo sample of recoil protons was obtained by generating diffractive events of the type $\gamma p \to p\eta'$ and simulating the response of the BSD in *Gradphi*. Which reaction is used is immaterial, from the point of view of the proton spectrum, because it depends only on the mass of the photoproduced system and the diffractive slope. For this simulation I used a diffractive slope $b = 8$ GeV^{-2}. The event generation takes into account the Fermi motion of the nucleon inside the ^{9}Be nucleus. The pulse height spectrum of the recoil protons in the BSD is shown in Fig. 3. More precisely, the lowest energy loss in the three BSD layers is plotted in the figure. This is the parameter on which a cut is made to simulate raising the discriminator threshold in triple-coincidence logic. The corresponding least-of-three energy loss spectrum for the background is shown in Fig. 4.

Comparison of these two spectra shows that a significant fraction of the background may be rejected at a minimal cost in recoil proton detection efficiency simply by raising the pulse height threshold on the BSD. This is quantified in Fig. 5. Since the BSD rates are dominated by background, the red curve can be taken to be proportional to the total level 0 trigger rate. The normalization is that of Table 1. The blue curve represents the fractional loss in recoil proton detection efficiency as a function of BSD threshold. It is clear from this plot that a reduction of a factor of 6 in the level 0 rates can be obtained by raising the BSD threshold before reaching the end of the recoil proton efficiency plateau. This calculation indicates that by balancing the gains of the BSD counters and adjusting the threshold to twice the minimum ionizing edge, the trigger rates will be comparable to what was obtained with the RPD. A further safety factor of 2-3 in rate reduction can yet be obtained by further raising the threshold before significant efficiency losses are encountered.

It should be kept in mind that the BSD recoil proton trigger is collecting 2.5 times more recoil protons than formerly did the RPD, simply because of the increased angular coverage. The laboratory angular distributions of the recoil protons and background tracks, respectively, are shown in Figs. 6-7. For contrast, the recoil proton angular distribution is shown in Fig. 8 for a hydrogen target. The peak position in Fig. 8

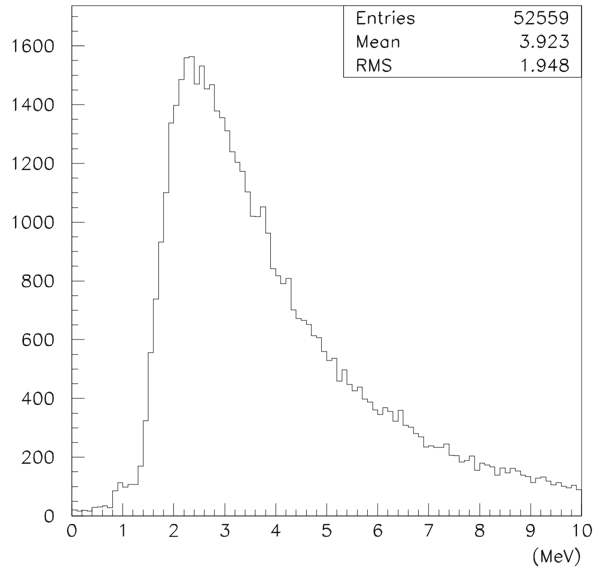

Figure 3: Energy loss spectrum for recoil protons from the diffractive photoproduction reaction $^{9}\mathrm{Be}(\gamma, p\eta')\,^{8}\mathrm{X}$. All three layers are required in coincidence and only the lowest of the signals in the three BSD layers is entered in this histogram. This is a Monte Carlo spectrum.

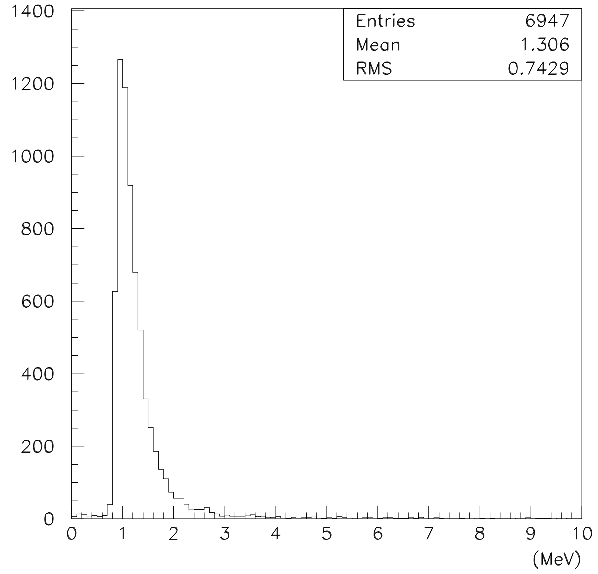

Figure 4: Energy loss spectrum for background tracks in the BSD. All three layers are required in coincidence and only the lowest of the signals in the three BSD layers is entered in this histogram. This is a Monte Carlo spectrum.

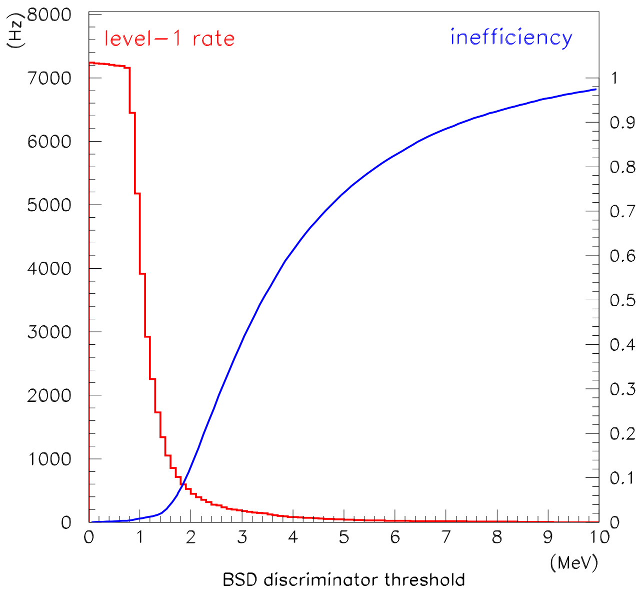

Figure 5: Total BSD triple coincidence counts in Monte Carlo run 1999a *vs* discriminator threshold (red curve, left axis) and inefficiency for triggering on recoil protons from diffractive photoproduction (blue curve, right axis).

is sensitive to the mass of the photoproduced meson, the η' in this case. This figure is presented to show the importance of the kinematic broadening due to the Fermi motion of the proton inside the nuclear target. The most important gains in recoil proton acceptance have been obtained at forward angles, where the background is also the highest. It appears fortuitous that the end of the scintillator barrel is located close to where the tradeoff between background and acceptance is turning over.

5 Trigger Timing

As a byproduct of this study, shown in Fig. 9 is the time of flight distribution for recoil protons from the reaction ${}^{9}\mathrm{Be}(\gamma, p\eta')\,{}^{8}\mathrm{X}$. Only hits from 60^o to 90^o in polar angle have been included so that all tracks have about the same path length from the target to the scintillators. The time-of-flight r.m.s. spread of about 700ps comes almost entirely from the velocity spread of the protons. From this plot one can judge what time resolution is needed for the BSD readout. The multi-hit TDC (LeCroy 1877) with a specified r.m.s. resolution of 400ps is quite adequate, and the improvement to be had with a high-resolution TDC for these events is marginal.

6 Predictions

In this section I convert the Monte Carlo numbers into predictions for the rates in each level of the Radphi trigger. The calculation relies on the model for the Radphi trigger presented in a previous note [1]. The parameters of the model were carefully calibrated using measurements taken during 1998 parasitic running. These parameters are carried over without change for this study, except that the rate in the UPV has been lowered by a factor of 5 to account for its having been moved upstream of its former position. The basic rate for the BSD triple-coincidence is taken to be the same as was measured for the RPD coincidence in 1998. Accidental coincidences between BSD layers are incorporated in addition to the basic "pixel" rate. The results are shown in Table 3. The BSD threshold was set at the maximum of the minimum-ionizing peak to obtain the reduction from the inclusive rates shown in Table 1. The difference between *actual* and *scaler* rates have to do with the dead time correction associated with each signal. For detector *or* signals,

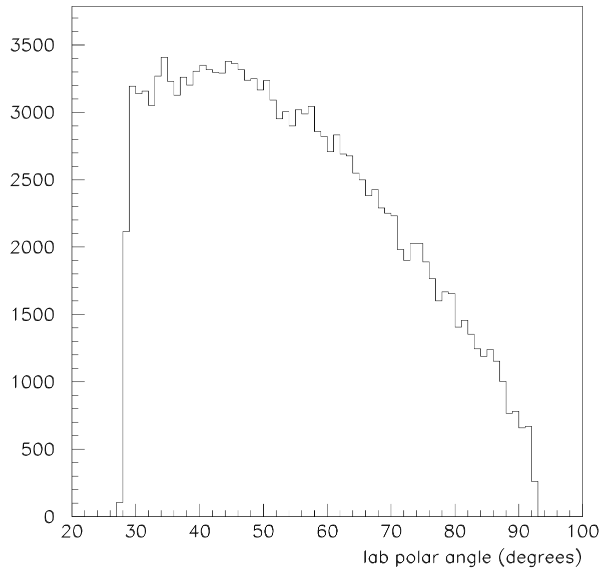

Figure 6: Lab polar angle distribution of recoil protons detected in the BSD during Monte Carlo simulation of the photoproduction reaction $^9\mathrm{Be}(\gamma, p\eta')\,^8\mathrm{X}$.

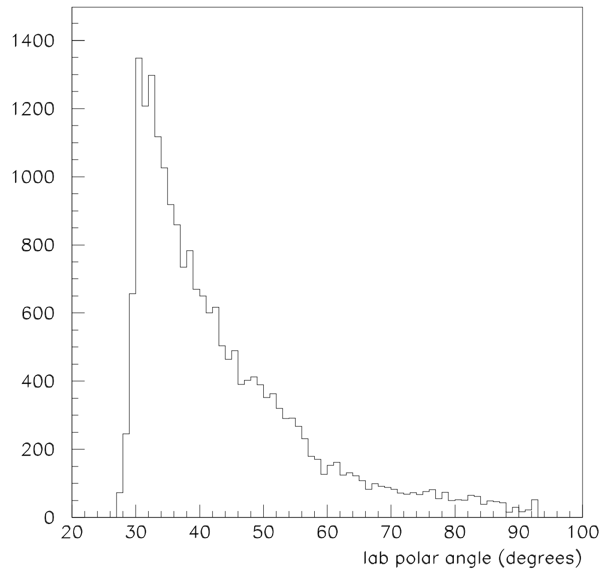

Figure 7: Lab polar angle distribution of triple coincidence triggers in the BSD during Monte Carlo simulation run 1999a. This distribution is dominantly low-energy electromagnetic background.

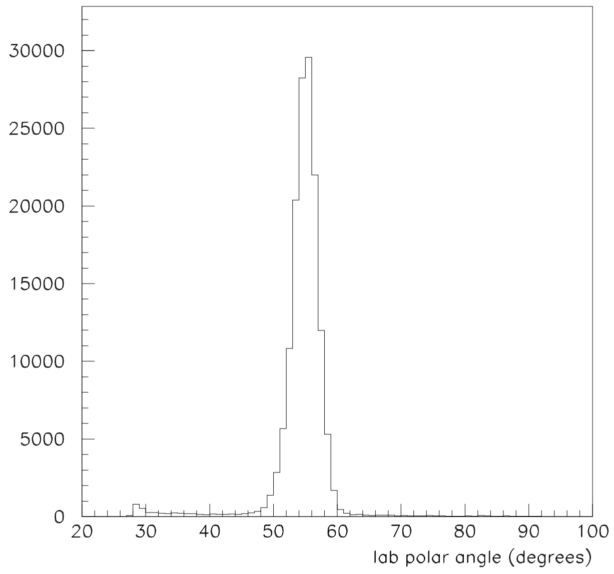

Figure 8: Lab polar angle distribution of recoil protons detected in the BSD during Monte Carlo simulation of the photoproduction reaction $(\gamma, p\eta')$ on a hydrogen target.

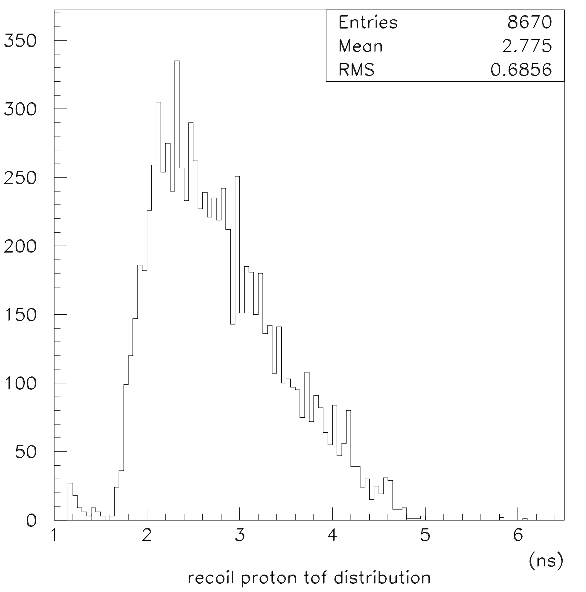

Figure 9: Time of flight distribution for recoil protons from the reaction ${}^{9}\mathrm{Be}(\gamma, p\eta')\,{}^{8}\mathrm{X}$. Only hits between polar angles of 60^o and 90^o are included in this spectrum.

Table 3: The rates expected in all levels of the Radphi trigger from the front end to the tape, based upon measurements taken during 1998 running and this study. All rates are normalized to running with 50nA electron beam at 5.5GeV energy and a $5 \cdot 10^{-4}$ radiation length radiator.

signal	actual	scaler
tagger *or*	48 MHz	30 MHz
CPV *or*	67 MHz	34 MHz
UPV *or*	750 KHz	740 KHz
BSD layer 1	3.9 MHz	3.8 MHz
BSD layer 2	2.0 MHz	2.0 MHz
BSD layer 3	1.2 MHz	1.2 MHz
BSD layer $1 \cdot 2$	1.1 MHz	1.1 MHz
BSD layer $1 \cdot 3$	590 KHz	590 KHz
BSD layer $2 \cdot 3$	590 KHz	590 KHz
BSD $1 \cdot 2 \cdot 3$	440 KHz	440 KHz
$BSD \cdot \overline{UPV}$	390 KHz	390 KHz
level 1 trigger	73 KHz	150 KHz
level 2 trigger	8.3 KHz	8.3 KHz
level 3 trigger	1.0 KHz	1.0 KHz
level 2 dead time	1.2 μs/event	(9%)
level 3 dead time	14 μs/event	(12%)
daq dead time	300 μs/event	(30%)
total live time	50% @ 1KHz	

the scaler rates are suppressed relative to the actual rates because the signals have a finite duration and the scaler only counts lead edges. For the level 1 trigger rate the scaler does not reflect the dead time imposed by the $BUSY$ signal, whereas the actual rate does.

Running an experiment with 50% live time is not unreasonable, as can be seen from Fig. 10. This plot shows the rate at which signal is being written to tape. What is meant by *signal* can be illustrated by a simple analysis in which all events with charged tracks (besides the recoil proton) are removed and then the time between the trigger and the tagger is plotted for the remaining events. In this plot appears a peak reflecting prompt coincidences surrounded by accidental background. The statistics in the coincidence peak, after accidentals are subtracted, is what is meant by *signal*. Of course the separation of signal from non-signal is only possible on a statistical basis. But in a tagged photon beam it is this quantity shown in Fig. 10 that is the figure of merit as far as statistics are concerned. This graph shows that the experiment profits from increased beam current all the way to 50nA, where it saturates.

7 Hadronic Component

The component of the background rates coming from untagged hadronic interactions of the beam in the target has been ignored in this discussion. I will argue here that for the purposes of calculating trigger and event rates it can be ignored. The hadronic interactions of a bremsstrahlung beam with a beryllium target must be analyzed over the full range of photon energies. By far the most important hadronic interaction from the point of view of sheer rate is nuclear photodisintegration. This cross section reaches a peak on the order of mb in the region of the giant resonances (10-30MeV) in most stable nuclei. Beryllium has a photodisintegration peak at very low energy (1MeV) [3] that has important implications for nuclear reactions inside stars. However for our purposes these interactions are not important; in spite of their copious production inside our target, the protons and alpha particles from photodisintegration are stopped before they escape the target. The neutrons that are released can escape the target, but their interaction probability in the thin trigger scintillators is small.

The most important hadronic interactions of the beam that contribute to background rates in the detectors is nucleon resonance photoproduction followed by pion emission. The $\Delta(1230)$ is the most important,

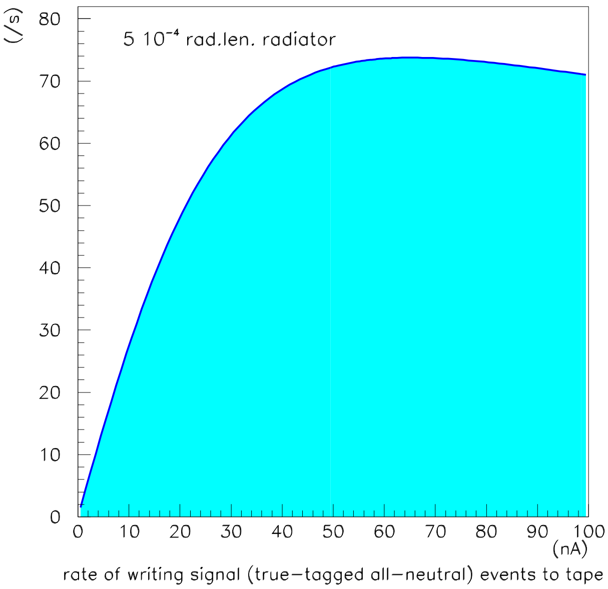

Figure 10: Predicted rate of writing good triggers to tape *vs* electron beam current for a $5 \cdot 10^{-4}$ radiation length radiator.

amounting to approximately 70KHz at a tagged rate of $5 \cdot 10^7 \gamma$/s. The higher lying N^* resonances contribute about 60KHz in addition. This covers the photon energy range up to about 2GeV. Above 2GeV the cross section becomes approximately constant at about 120μb. Here the interactions are diffractive in character and contribute about 30KHz to the total rate in the detector, 6KHz of which is tagged. These numbers include only reactions with a recoil proton; to obtain an inclusive rate that covers reactions with a recoil neutron as well, they should be multiplied by 9/4.

Comparison with the singles rates in Table 3 shows that the hadronic component is a small fraction of the total, of order 10% at best. Most of the hadronic tracks in an inclusive sample come from charged pions, and these are suppressed at the same time as the electromagnetic background by raising the threshold on the recoil proton trigger scintillators. With a dE/dx suppression factor of 5 and a tagger accidental probability of 40%, this brings the total hadronic rate to about 30KHz. Delta resonance decays favour neutral pion over charged pion production 2:1, so averaged over the entire spectrum this gives a further reduction in the inclusive hadronic trigger rate of a factor of about two. This leads to 15KHz of level 1 triggers from hadronic events, to be compared with 150KHz in Table 3 for electromagnetic sources. Only a fraction of this hadronic rate is within the acceptance of our recoil proton trigger.

Beyond level 1, most of these events are eliminated by their low energy deposited in the LGD. What remains at this point is essentially just the diffractive neutral events from the tagged end of the photon spectrum. The rates calculation presented in this report included 3KHz of tagged hadronic events in the trigger at level 1, two thirds of which contain charged tracks in the forward region. These events are kept at level 2 but get reduced at level 3 by about a factor of 10 by the requirement total energy requirement in the forward calorimeter. All of these ratios were extracted from the data taken during 1998 running. That one sees 3KHz at level 1 instead of 6KHz follows from the fact that the RPD trigger saw only a fraction of the total recoil protons. With the BSD one might expect this number to increase closer to the full acceptance limit of 6KHz. This would have a negligible impact on the rate of events written to tape because the events passing the level 3 trigger are 90% accidentals at full beam intensity. I conclude that the uncertainty in these predictions from hadronic backgrounds that have not been taken into account amounts to about 5% which justifies having disregarded them in this study.

8 ADC Gate Width

One of the conclusions from this study is that the backgrounds in the Radphi experiment are mostly soft electromagnetic debris. The gamma ray flux is more intense than that of the e^+e^- component at low energies (a few MeV) by a factor of roughly 3. However the charged particle spectrum is harder than the X-rays, so that at energies above 50MeV, the background is mostly charged particles. These charged tracks are most intense at low angles, but their distribution reaches out far enough to cause concern about pileup effects in the LGD. This section presents quantitative estimates of these effects.

There are two effects we can expect from pileup: degraded resolution from blocks that are part of a cluster, and extra clusters. First I consider the effects of degraded resolution. These can be estimated simply by looking at the ADC spectrum of a block that does participate in a cluster. This "pedestal" distribution is implicitly convoluted with the measured energies blocks that do participate in a cluster, so it is there whether or not the block is hit. By looking at the pedestal distribution for blocks far from a shower center, the measurement error from pileup can be observed directly. In Fig. 11 is shown the pedestal distribution for one of the 8 blocks closest to the photon beam axis. The tail on the high side of the peak comes from accidental coincidences between the event trigger and an uncorrelated hit (mostly electron/positron tracks) that falls within the ADC gate. The gate is assumed to be 250ns wide. The tail on the low side of the peak comes from accidental coincidences between the event trigger and an uncorrelated hit (mostly electron/positron tracks) that falls within the pre-sampling interval used by the ADC to set its zero. This pre-sampling interval is assumed to be 50ns in the Monte Carlo simulation.

The same distribution is shown in Fig. 12 for blocks that are adjacent to the 8 innermost LGD blocks. The intrinsic width of the pedestal was set to 10MeV (electronic noise) in the simulation. These plots are similar to what was shown by Scott Teige from data taken during 1998 running. From them we can conclude that pileup is most significant for the inner blocks, as expected. What is not so obvious from just looking at Fig. 12 is that the r.m.s. of the pedestal is more than doubled by the background, the effect of the broad wings under the peak. Once 6 or 7 blocks with such pedestals are added together, the residuals become Gaussian and are determined only by the r.m.s. of the constituent measurements, and not by the f.w.h.m., for example. Thus, we can expect pileup effects to determine the limiting resolution of the LGD for showers in the central region. A figure for tier-3 blocks is not shown, but the pedestal r.m.s. for blocks in that region was determined to be broadened from 10MeV to 14MeV by pileup. Beyond tier-3 pileup can be assumed to be negligible. This also implies that one can neglect pileup effects in the BGV.

The degradation of LGD resolution from pileup in the inner few tiers of blocks can be ameliorated by reducing the width of the ADC gate. At this point it is not possible to reduce the pre-sampling interval below its present value of 50ns. However, if the gate width is reduced from 250ns to 125ns, the r.m.s. width of the pedestal is reduced by a factor of 1.5.

The second effect from pileup has much more serious implications for the experiment. Since there is no timing information from the LGD wall, all hits in the lead glass that occur within the interval of the ADC gate must be considered to be a part of the event. Let it be presumed that a given set of clusters constitutes a desirable event, according to some analysis criteria. That event will be spoiled by *any* hit, charged or neutral, above the cluster-energy threshold that occurs within the ADC gate. As mentioned previously, the hard part of the background is essentially all electron/positron tracks below 15^0. The rate for these is considerable, as can be seen from Table 4. The rate of clustered centered in the innermost blocks has been listed separately because these blocks are treated differently by the cluster finder. But even excluding these blocks, these numbers indicate that pileup of charged shower clusters within the ADC gate makes a real difference in terms of our acceptance.

This acceptance deficit from pileup in the LGD has not been included in the calculation of total signal to tape presented earlier in this note. Since the effect is rate-dependent, in principle it should be included, because it is the number of reconstructible events that one would like to optimize by adjusting the beam intensity. However, it is possible for us to decrease the ADC gate and diminish the pileup effects. Reducing the fractions in Table 4 by a factor of 2 would make a significant difference to the statistics of reconstructed events collected by the experiment. I propose that tests be made early during the 1999 run period, with a goal of reducing the ADC gate width to the vicinity of 100ns.

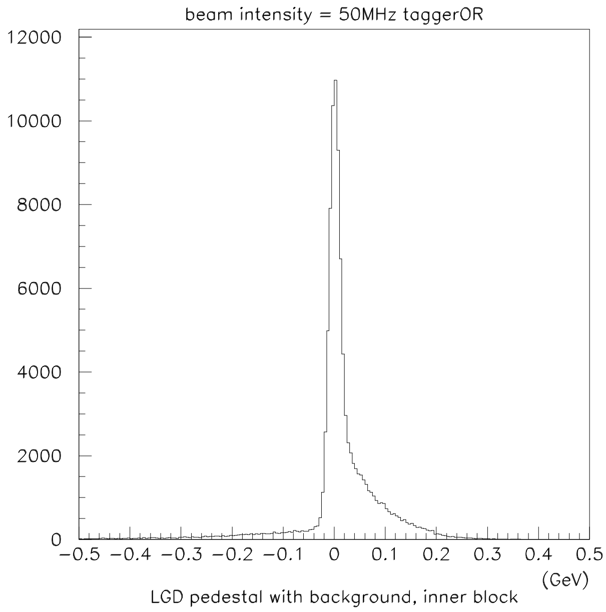

Figure 11: Pedestal distribution from Monte Carlo for one of the eight LGD blocks that are closest to the photon beam axis. The r.m.s. of the pedestal is 80MeV.

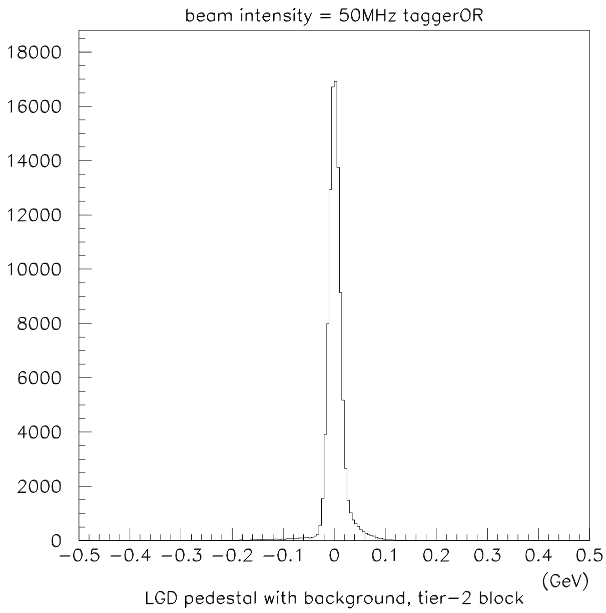

Figure 12: Pedestal distribution from Monte Carlo for LGD blocks that are adjacent to the eight inner LGD blocks. The r.m.s. of the pedestal is 25MeV.

Table 4: Fractions of otherwise reconstructible events in any given channel that are poisoned by extra clusters that appear in the LGD due to uncorrelated background that falls within the ADC gate width of 250ns. The threshold indicates what minimum initial energy a e^+/e^- particle must have on entry to the LGD in order to produce a shower that will be found by the cluster finder.

	average number of accidental clusters	
threshold	everywhere	excluding inner 8 blocks
70 MeV	1.35	0.45
100 MeV	0.65	0.19
150 MeV	0.25	0.07

References

[1] "Prospects for running Radphi at design luminosity in 1999", R.T. Jones, Technical Note *radphi-1998-901*, October 24, 1999.

[2] **Gradphi** is a Monte Carlo simulation of the Radphi apparatus and beam line that was developed by A. Kurylov and others. It is ready and available for use under the CVS software repository for this experiment.

[3] "Low-energy photodisintegration of ^{9}Be and $\alpha + \alpha + n \rightarrow^9$ Be $+ \gamma$ reactions at astrophysical conditions", V.D. Efros et.al, *nucl-th/9802024*, 1998.